Proceedings of the 39th IAHR World Congress
19-24 June 2022
Granada, Spain
DOI number

Effects of Highly Transient Boundary Conditions on Groundwater Solute Transport

Mónica Basilio Hazas[1] and Gabriele Chiogna[1]

[1] Technical University of Munich, Munich, Germany
monica.basilio@tum.de

Abstract

Spreading, dilution and mixing processes in the groundwater are influenced not only by the heterogeneous properties of the porous media but also by the boundary conditions. Although less studied than the heterogeneity of the soil matrix, highly transient boundary conditions can often occur in the field and can also enhance mixing in Darcy flows. In this work, we focus on surface water-groundwater interaction, in particular on rivers affected by hydropeaking, an artificial flow regime with sharp and frequent water level fluctuations resulting from the operation of hydropower plants. To study how hydropeaking can affect the groundwater flow field and thus mixing in the subsurface, we modeled a cross-section of the Adige Valley, in Italy, where two Alpine rivers, the Noce and the Adige, are differently affected by hydropeaking. We performed two-dimensional flow and transport simulations using a calibrated model, and investigated different scenarios, considering both sub-daily and seasonal fluctuations. We characterized the flow field applying different topological and kinematic indicators and show their relation to mixing processes in the subsurface. Our results show that hydropeaking and hence the management of hydropower plants have a major effect on groundwater solute transport.

Keywords: Hydropeaking; Groundwater; Solute transport; Riverbed

1. INTRODUCTION

Natural groundwater systems may be connected to fluctuating surface water bodies, water sinks and source terms which lead to transient boundary conditions. These conditions, together with the heterogeneous properties of the porous media, affect spreading, mixing and dilution processes in the aquifers (Rolle & Le Borgne, 2019). While some transient boundary conditions are due to natural factors, such as ocean tides (Geng et al., 2020; Trefry et al., 2019) and seasonal fluctuations as occurs in rivers controlled by glacier melting (Pérez Ciria et al., 2019), others changes are caused by anthropogenic factors, including engineered pumping systems (Cho et al., 2019; Neupauer et al., 2014) and water management, in particular hydropeaking, an artificial flow regime characterized by changes in the water level due to the operation of hydropower plants (Ferencz et al., 2019; Arntzen et al., 2006).

Several works have shown the effects of hydropeaking on the hydrological cycle and sediment transport (Bruno et al., 2009; Fette et al., 2007), the physicochemical characteristics of the water (Hauer et al., 2017; Zolezzi et al., 2011), and the interaction with hyporheic water (Singh et al., 2019; Song et al., 2018; Sawyer et al., 2009), with mostly negative impacts for riverine ecosystems (Bejarano et al., 2018; Casas-Mulet et al., 2021). Beyond the hyporheic zone, hydropeaking can cause variations in the groundwater level in river corridors and riverine islands (Francis et al., 2010; Song et al., 2020), and influence the transport of dissolved solutes near the shore (Zachara et al., 2016). More recently, an experimental study at laboratory scale by Ziliotto et al. (2021) has shown that hydropeaking has the potential to enhance the dispersion and spreading of a conservative plume moving below two rivers in a homogenous aquifer.

Understanding mechanisms behind mixing enhancement is relevant because mixing is slow in porous media and reactions are often incomplete (Valocchi et al., 2019; Wright et al., 2017), thus hindering the degradation of contaminants in the groundwater. In general, variations in the magnitude and direction of the velocity can increase mechanical dispersion, stretching and folding therefore enhancing mixing (Neupauer et al., 2020; de Anna et al., 2014). While these velocity variations are generally due to heterogeneities and anisotropies in the porous media (Ye et al., 2020; Cirpka et al., 2015), they can also be caused by transient boundary conditions (Piscopo et al., 2013; de Dreuzy et al., 2012; Dentz & Carrera, 2005). In fact, injection-extraction systems (Neupauer et al., 2014; Sposito, 2006) and tidal forcing (Wu et al., 2020; Trefry et al., 2019) can generate transient flow fields with a complex and chaotic mixing dynamics.

The interaction between transient boundary conditions and heterogeneity and their effect for solute transport has been studied for different groundwater scenarios; for instance, de Dreuzy et al. (2012) for uniform fluctuations, Neupauer et al. (2014) for engineered systems, and Geng et al. (2020) for coastal aquifers. In terms of river-aquifer systems, Cardenas et al. (2004) analyzed the effect of heterogeneity in the hyporheic zone

with its geometry, and Song et al. (2018) studied the impact of hydropeaking on the thermal regime and the biogeochemical reactions of a heterogenous cross-section of the hyporheic zone. In this work, we aim to study the interaction between river stage fluctuations and the heterogeneity of an aquifer, considering the conductivity of the river bed. For this, we model a cross-section of an aquifer located in an Alpine valley that is traversed by two rivers differently affected by hydropeaking, and perform flow and transport simulations with seasonal (daily resolution) and sub-daily (hourly resolution) fluctuations. We explore therefore, the effects of such fluctuations on a conservative tracer plume by analyzing its spatial distribution and dilution index, under different hydraulic scenarios.

2. METHODOLOGY

2.1 Study area and model

We study the aquifer under the Adige Valley (north of Italy), in particular the area between Mezzolombardo and San Michele all'Adige (Figure 1a). The valley is composed by loose sediments from the alluvial fan formations of the Adige River and its tributaries, and to the east and west is bordered by calcareous dolomitic mountains. Originally a wetland, the area has a high demand of groundwater for irrigation of vineyards (Castagna et al., 2015). As in most Alpine catchments, its hydrological regime is characterized by snow and glacier melting in spring, however it is heavily impacted by hydropeaking (Chiogna et al., 2016).

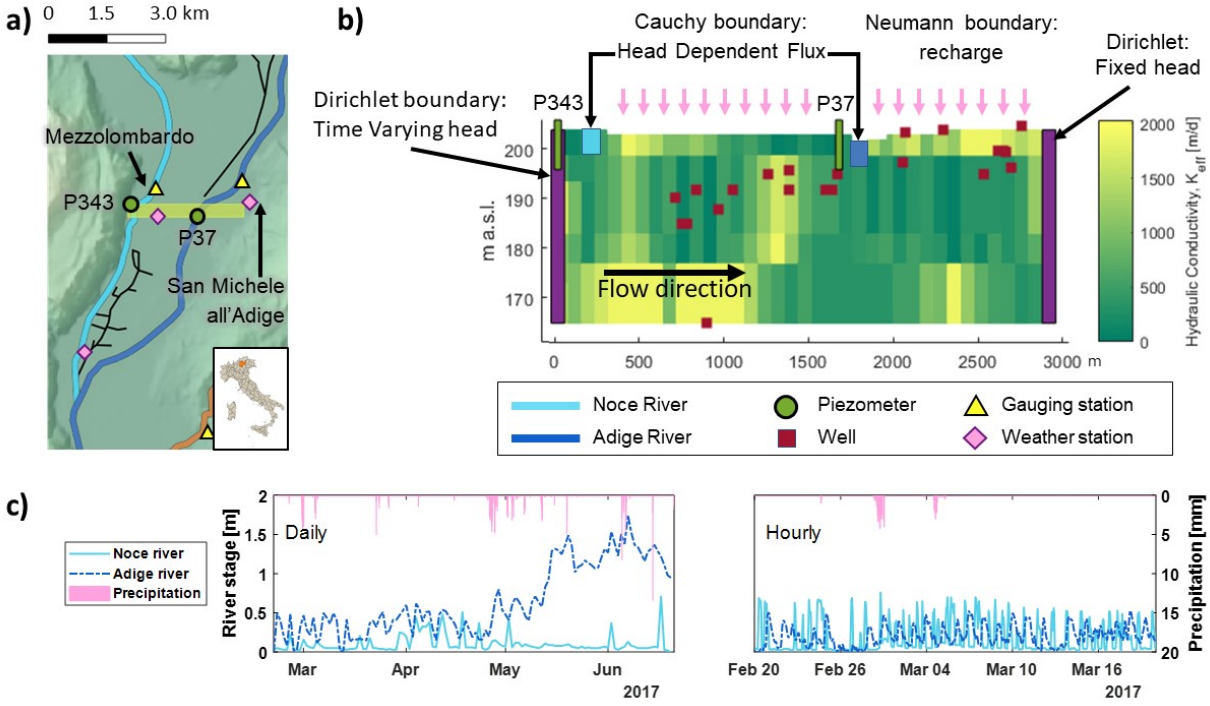

Figure 1. a) Modeled area in the Adige Valley; b) model and hydraulic conductivity of the cross section; and c) hydrograph at daily and hourly timescales with precipitation.

Figure 1b shows the modeled vertical cross-section of the Adige Valley, which is traversed by the Adige River and the Noce River, a tributary of the Adige. The model origin is at long= 661636.44 and lat=5117317.54 (WGS84 – UTM 32N). The bottom of the unconfined aquifer is at 164 m a.s.l. and the topographical elevation of the surface varies from 204 to 209 m a.s.l. From west to east, the model extends of approximately 3120 m. The model is therefore discretized in 780 columns of $\Delta x = 4$ m and 80 layers of $\Delta z = 1$ m. Overall, we follow the methodology used in (Castagna et al., 2015) to model a larger section of the Adige Valley, and we consider the hydraulic conductivity field which is used by the Geological Survey of Trento. The left and right sides of the cross-section are Dirichlet boundary conditions. On the left, we use the measurements of the piezometer P343 to implement a time variant specified head, and on the right, we apply a constant head. This boundary is far from the areas close to the highly transient boundary conditions (i.e. rivers) and it does not affect significantly the transient model.

On the top of the model, we apply Cauchy boundary conditions to implement the aquifer's recharge, which is computed after a leakage model based on soil saturation moisture (Laio et al., 2001; Rodriguez-Iturbe et al., 2001). Precipitation data was obtained from the meteorological stations at Mezzolombardo (Meteotrentino, 2022) and San Michele all'Adige (3BMeteo, 2022). Precipitation at Mezzolombardo aggregated for daily steps

is shown in the top axis of Figure 1c. Evapotranspiration and irrigation were obtainned from (Galli, 2019). We assign the recharge to each cell after the Thyesen polygon method. Cauchy boundary conditions were also applied to introduce the pumping wells. In fact, the cross-section contains several pumping wells, which location, use and maximum allowed pumping rate were provided by the Geological Survey of Trento. The rivers are implemented as Neumann boundary conditions, or head-depending flux. To estimate the river stage, we collect hourly data from the gauging stations of Mezzolombardo Ponte Rupe and San Michele all'Adige, provided by the Dam Office of the Autonomous Province of Trento (Provincia Autonoma di Trento - Ufficio Dighe, 2017). We calculate the stage at the model area using the Chézy equation under the assumption of a rectangular channel and that the river flow is constant between the gauging stations and the area of interest. We consider a model at daily resolution to consider weekly and seasonal fluctuations, and a model at hourly resolution to account for sub-daily fluctuations. The daily resolution simulation is from February 20th to May 20th, 2017, while the hourly resolution simulation is for a one-month period, from February 20th to March 20th of the same year. The hydrograph of the Noce and the Adige rivers for both daily and hourly models is shown in Figure 1c.

2.2 Model calibration and synthetic scenarios

We calibrate the specific yield and the vertical hydraulic conductivity of both the Noce and the Adige riverbeds, and adjust the bottom of the riverbed at the Adige. For this, we use a Montecarlo approach and apply as objective functions the mean average error (MAE), and root mean squared error (RMSE), and the Nash-Stutcliffe coefficient (NSE). Piezometer P37 is used as calibration point. We calibrate the model at daily resolution (MAE=0.05, RMSE=0.07, NSE=0.98 and validate it with the hourly resolution (MAE=0.02, RMSE=0.03, NSE=0.85). In addition to the calibrated model, we simulate synthetic scenarios to account for the broad range of values in the hydraulic conductivity of the riverbed (Tang et al., 2015), as well as the case of a steady river stage. Therefore, we consider the cases of the vertical hydraulic conductivity k of the river as follows: 0.01k, 0.1k, 0.2k, 0.5k and 10k for the transient models, and k for the steady state simulation, where k is the calibrated hydraulic conductivity. For comparability purposes between the simulations at daily and hourly resolution, the steady state simulation uses the mean groundwater and river heads of the hourly model (February 20th - March 20th, 2017).

2.3 Groundwater flow and transport equations

The groundwater flow equation for a representative volume can be described by a combination of the Darcy's law with the continuity equation

$$S\frac{\partial h}{\partial t} = \nabla \cdot (-\boldsymbol{K} \cdot \nabla h) + \boldsymbol{q}' \qquad [1]$$

where $\mathbf{K}\ [LT^{-1}]$ corresponds to the hydraulic conductivity tensor, $\nabla h[-]$ is the hydraulic head gradient, $\boldsymbol{q}'[LT^{-1}]$ accounts for the source and sink, and $S\ [-]$ is the storage coefficient. We solve the groundwater flow equation with the finite differences code MODFLOW-OWHM (Boyce, 2022). Specifically, we apply the Newton-Raphson solver (Niswonger et al., 2011), which is recommended for cases with water table fluctuations across different layers.

The rivers were implemented using the river package of MODFLOW. As mentioned earlier, the model is calibrated for the vertical hydraulic conductivity k of the river beds. This parameter is introduced in the river package through the riverbed conductance, defined as

$$C = \frac{\Delta \mathrm{x} \Delta \mathrm{y} k}{M}, \qquad [2]$$

where $\Delta \mathrm{x}$ and $\Delta \mathrm{y}$ are the length and width of the cell occupied by the river, and M is the thickness of the riverbed. We assume a thickness of 1 m in order to calculate the vertical hydraulic conductivity k from the calibrated riverbed conductance.

The transport of solutes is solved by the advection-dispersion equation (ADE). For a conservative tracer, the advection-dispersion equation is written as

$$\frac{\partial (nC)}{\partial t} = \nabla \cdot (n\boldsymbol{D}\nabla C) - \nabla \cdot (n\boldsymbol{v}), \qquad [3]$$

being $C[\mathrm{ML}^{-3}]$ the tracer concentration, $n[-]$ the porosity, and $\boldsymbol{D}[\mathrm{L}^2\mathrm{T}^{-1}]$ the dispersion tensor. We solve the ADE using MT3D-USGS (Bedekar et al., 2016). The dispersion tensor uses a longitudinal dispersion coefficient, D_L, while the transverse dispersion coefficient is parametrized as $D_T = 0.1D_L$.

2.4 Dilution Index

We use the dilution index (Kitanidis, 1994) to evaluate mixing for the solute concentrations estimated with the ADE. The dilution index is understood as the exponential of the entropy of the system, defined by

$$E(t) = \exp\left[-\int_V p\,(\boldsymbol{x},t)\,ln\,p(\boldsymbol{x},t)\,dV\right], \quad [4]$$

where $p\,(\boldsymbol{x},t)$ is the mass probability density function of the concentration at the coordinates $\boldsymbol{x}$, at time t in a system of volume V, and it is calculated by

$$p(\boldsymbol{x},t) = \frac{C(\boldsymbol{x},t)}{\int_V C\,(\boldsymbol{x},t)dV}, \quad [5]$$

Higher values of the dilution index correspond to a better dilution of the system.

3. RESULTS AND DISCUSION

3.1 River fluctuations and groundwater heads

We start the analysis with the model at daily resolution, which requires a simulation time much lower than the model at hourly resolution (less than a third), and in the area of the Noce River. In addition to the field observations, we added observation points for the simulated groundwater heads below the river and 25 m before the first river cell. During most of the simulated period, the estimated river head of the Noce is higher (0.15 ± 0.15 m) than the measured groundwater head at piezometer 343, located 95 m to the left of the river. Compared to the groundwater head below the river, the Noce is 0.06 ± 0.03 m higher, indicating that the Noce River is feeding the aquifer. On the side of the Adige River, the estimated river head is 0.36 ± 0.06 m lower than the groundwater head at piezometer 37 (85 m from the river), and the groundwater level below the riverbed is 0.01 ± 0.008 m higher than the river head, indicating that at the studied cross-section, the aquifer is feeding the river, and the groundwater flows towards the Adige.

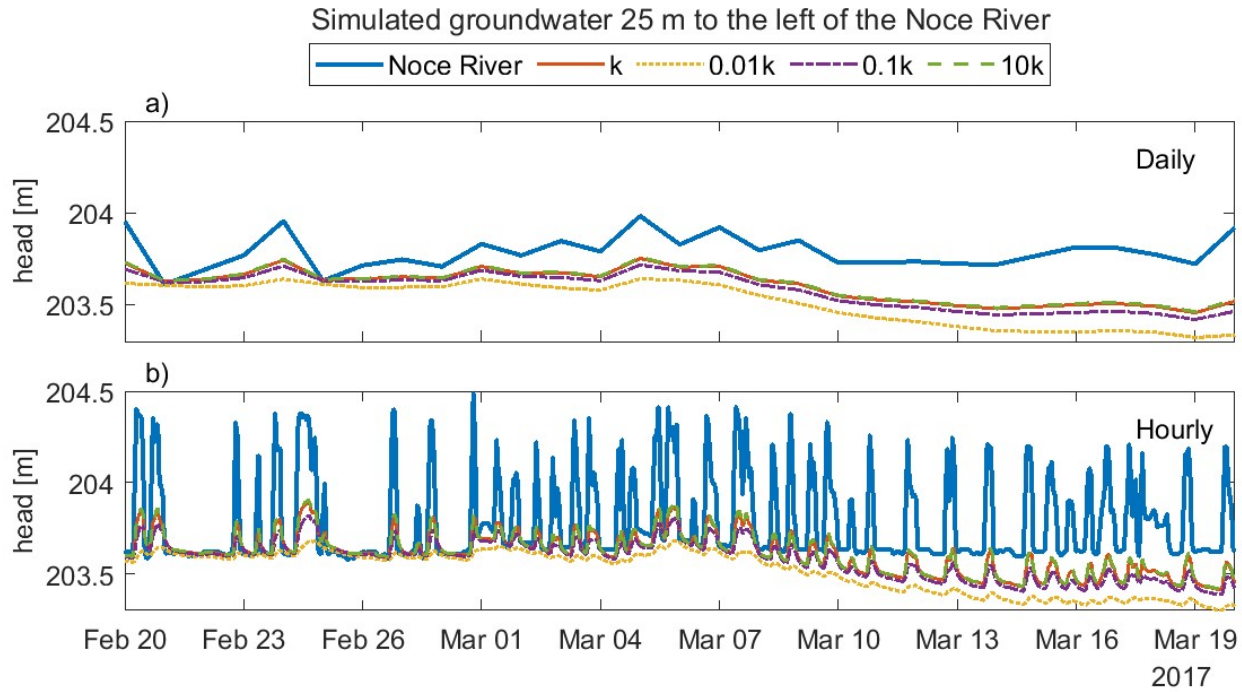

Figure 2. River fluctuations and simulated groundwater heads for the model at a) daily and b) hourly resolution for calibrated and synthetic scenarios during one month.

As a comparative example of the simulated groundwater heads in the calibrated model and selected synthetic scenarios, we show in Figure 2a the case for the daily observation points placed 25 m to the left of the Noce River during the period from February 20th to March 20th, 2017. We also included the estimated river head

at the cross-section. The simulated groundwater levels are highly dependent on the boundary conditions, as it is noticeable in particular after March 7th, when the groundwater head drops. However, it is also possible to observe changes in the groundwater due the river fluctuation, as the tough in February 21st or peaks in February 24th and March 5th, in particular for k and 10k.

3.2 Interplay of hydraulic conductivity, river fluctuations and riverbed conductance

In order to study how solute transport is affected by hydropeaking in a heterogenous aquifer cross-section, we prepared the transport simulation in the seasonal model and considered a conservative tracer representing a contaminant plume with an initial rectangular shape 28 m length, 3 m wide and with a centroid placed 40 m to the left of the Noce River and 10 m below its riverbed. Its initial concentration is 100 [M/L^3].

As the plume starts moving, it is pushed towards the bottom of the aquifer due to the combined effect of the river stage higher than the groundwater and the hydraulic conductivity field. In fact, the hydraulic conductivity below the Noce is lower compared to the region below the tracer plume, forming therefore a preferential path in the vertical direction enhanced by the vertical component of the velocity. Once the plume reaches the bottom of the aquifer, it moves to the right direction through the area with high hydraulic conductivity (Figure 1b between 164 and 175 m a.s.l. and 0 and 1000 m in the longitudinal direction). The plume distribution and its concentration at the end of the simulation is seen in Figure 3a (left colorbar), the magnitude of the velocity field is shown as background (right colorbar), and the blue rectangle on the top indicates the location of the Noce river.

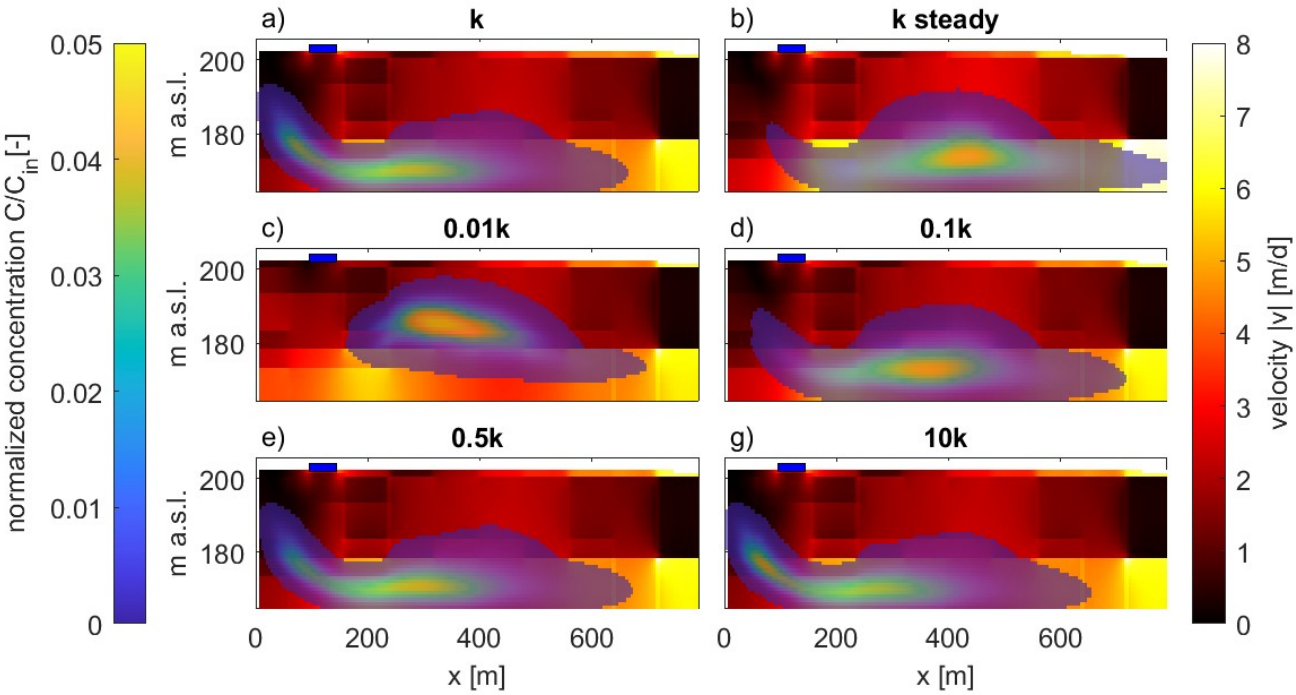

Figure 3. Magnitude of the velocity field and solute tracer distribution after 121 days for the calibrated transient model (a) and the synthetic scenarios (b-g).

The final plume distribution for the steady state simulation and the 0.01,0.1k,0.5k and 10 k scenarios is shown in Figures 3b-3g. These scenarios allow us to analyze the interplay of the heterogeneous conductivity field with the riverbed conductance and the river fluctuations. All the plumes have a hat/cap shape due to the fact that where the plume has a larger longitudinal dispersion in the area of higher velocity at the bottom of the aquifer. But they can also be grouped in different behaviors. For instance, the plumes of k, 0.5 k and 10 k (Figures 3a, 3e and 3g, respectively) look very similar at the first sight, and the simulated heads, compared below the river and at distances 25 and 40 m before the river, do not show a significant variation. However, the peak concentration of the plume is slightly different. In 0.5k, the peak is between 200 and 400 m, while in 10 k, the peak is between 50 and 100 m. In k, the concentration displays two local maxima in those two locations. A possible explanation is the interplay between the regional flow direction (to the right) and the feeding river that generates locally a flow in the opposite direction, that is, from the river to the left boundary. When k is higher, more water is exchanged between the river and the groundwater and the flow velocity towards the left boundary is higher, pushing the plume backwards.

The plumes k steady and 0.1k look similar to each other (Figures 3b and 3d). Like the first described group, they also move towards the bottom of the aquifer, but the peak concentration is not as stretched as for the

former three cases and it arrives further, around 380 m for 0.1k and 400 m for the steady state. A reason why k steady reaches a farther distance than 0.1k is that it is does not experience the fluctuations that can increase the flow direction backward and therefore delay the plume. The most different final tracer distribution is encountered for the case 0.01k (Figure 3c), which does not reach the bottom of the aquifer. Here, the magnitude of the velocity field below the Noce River is also different from the other cases. Due to the low riverbed conductance, the vertical velocity is not pushing the plume to the bottom of the aquifer and the plume moves rather horizontally. This case is representative for a clogged riverbed.

While the final plume distribution is different when the hydraulic conductivity of the riverbed varies in orders of magnitude, it is interesting to observe that the variations in the groundwater head at 25 from the river are minimal (e.g. Figure 2a). In fact, assuming that the results for k are a measured groundwater head, MAE ≤ 0.021, RMSE≤ 0.024 and NSE>0.9 for the scenarios $\geq$ 0.1k for the four months simulated period. Only the scenario of 0.01k gave poor statistical values. With respect to the calibration point, the riverbed conductance of the Noce river is less sensitive than the river bed conductance of the Adige river. Considering that the conductivity of the river bed can change significantly over short distance, it is important to be aware of the different possible scenarios and the low model sensitivity to the groundwater heads, in particular when modeling solute transport in a regional model under highly transient boundaries in this heterogeneous aquifer.

3.3 Sensitivity of dilution index at daily and hourly resolution

We extend the previous analysis of solute transport to the Adige river and to the simulations at hourly resolution by estimating the dilution index. As mentioned earlier, the hourly resolution accounts for the subdaily fluctuations typical of rivers under hydropeaking. First of all, we place an initial solute concentration near the Adige River at the same relative distance as the plume near the Noce River. Here, the plume moves towards the river and starts leaving the system after 15 days. To keep only the period in which the tracer is present only in the aquifer and for comparison purposes, we present in Figure 4 the dilution index for both time resolutions and both rivers during the first 15 days. Despite the differences found in the location and distribution of the tracer concentration in section 3.2, the dilution index reaches similar values for all the transient simulated scenarios (Figure 4a), only the steady state scenario displays a different dilution. The hourly simulations (Figure 4c), on the contrary, show a broader range of the dilution index. The lowest final dilution value is the same as in the daily simulation: the steady state scenario. However, the dilution index after 15 days increases as the vertical hydraulic conductivity of the Noce Rive increases. Considering hourly resolution rather than a daily one may be particularly important when analyzing contaminant plumes. For instance, a daily resolution model may show that a plume has already diluted to no-harmful concentrations, while the same model but at hourly resolution may reveal that the peak concentrations are still dangerous for the environment.

Similar to the analysis of the Noce, we compared the scenarios with the simulated head 25 m to the left of the Adige River for the hourly simulations (Figure 2b). The different riverbed conductances of the transient simulations are not sensitive to the groundwater head in that point (MAE<0.031, RMSE<0.032 and NSE>0.99), except for 0.01k (MAE=0.19, RMSE=0.21 and NSE=0.75), where the groundwater head is higher than the other cases, since less water from the aquifer goes into the river. At the calibration point, it is possible to notice changes in the simulated groundwater head, showing that the groundwater head propagation is also sensitive to the hydraulic conductivity of the riverbed. Unlike the plume near the Noce that is affected by the subdaily river fluctuations, the behavior of the dilution index of the plume near the Adige river is controlled by the advection forces leading the plume towards the river (Figures 4b and 4d). In fact, the dilution index looks almost the same for all transient scenarios and the steady state model, except for 0.01k. In this case, the low riverbed conductance leads to a lower velocity of the aquifer water feeding the river. Similar to the Noce, the hourly resolution also leads to larger values of the dilution index, and it increases the difference between the higher and lowest dilution value (0.01k in this case).

Overall, our results emphasize both the necessity to account for sub-daily fluctuations rather than using the mean daily values when studying solute transport in highly transient systems and the heterogeneous response of surface water –groundwater interaction in two rivers, both affected by hydropeaking under similar hydrological and geological conditions.

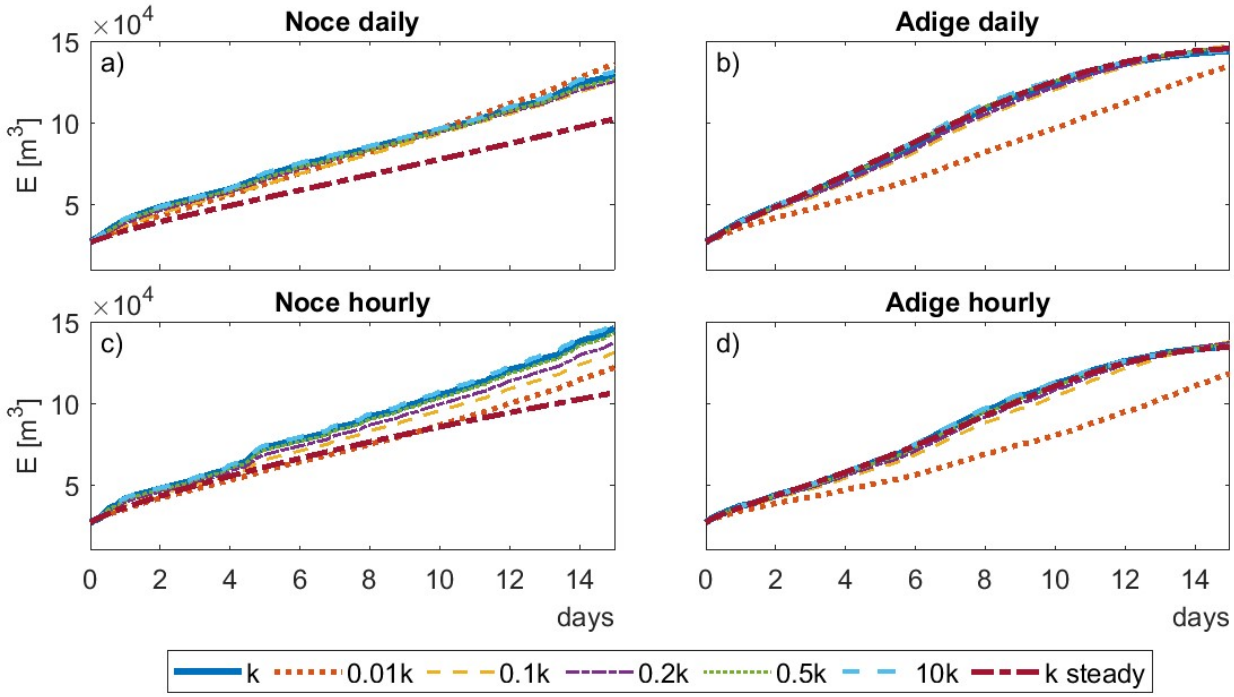

Figure 4. Dilution index for both rivers for the hourly and daily simulations during the first 15 days.

4. CONCLUSIONS

In this work, we modeled an aquifer cross-section of an Alpine valley differently impacted by two rivers affected by hydropeaking. We performed simulations at daily scale to consider seasonal fluctuations, and at hourly resolution to consider the effect of sub-daily fluctuationns. We compared scenarios with different hydraulic conductivity of the river bed by analyzing variations in the groundwater head, the distribution of a tracer plume and the dilution index. Our results show that in a natural system, the interplay between the river fluctuations, and of the hydraulic conductivity of the aquifer and of the river bed can lead to a complex transport dynamic. In particular, the effect of sub-daily river stage fluctuations can be a relevant to correctly quantify the dilution index of a plume passing close to the river.

5. ACKNOWLEDGEMENTS

This research is a result of the UNMIX project (UNcertainties due to boundary conditions in predicting MIXing in groundwater), which is supported by Deutsche Forschungsgemeinschaft (DFG) through TUM International Graduate School of Science and Engineering (IGSSE), GSC 81. We acknowledge the help provided by Marta Castagna, as well as Gianluca Tomasi from the Geological Survey of Trento. MBH also acknowledges the Mexican National Council for Science and Technology (CONACYT) and the Consejo Veracruzano de Investigación Científica y Desarrollo Tecnológico (COVEICYDET). Additional financial support for GC was provided by DFG (CH981/4-1, project Hydromix).

6. REFERENCES

3BMeteo. (2022). *Meteo mese, storico di San Michele All'adige 2017*. Retrieved from https://www.3bmeteo.com/meteo/san+michele+alladige/storico

Arntzen, E.V., Geist, D.R., & Dresel, P.E. (2006). Effects of fluctuating river flow on groundwater/surface water mixing in the hyporheic zone of a regulated, large cobble bed river. *River Research and Applications*, *22*(8), 937–946.

Bedekar, V., Morway, E.D., Langevin, C.D., & Tonkin, M. (2016). *MT3D-USGS version 1: A U.S. Geological Survey release of MT3DMS updated with new and expanded transport capabilities for use with MODFLOW.*

Bejarano, M.D., Jansson, R., & Nilsson, C. (2018). The effects of hydropeaking on riverine plants: a review. *Biological Reviews of the Cambridge Philosophical Society*, *93*(1), 658–673.

Boyce, S.E. (2022). MODFLOW One-Water Hydrologic Flow Model (MF-OWHM) Conjunctive Use and Integrated Hydrologic Flow Modeling Software, version 2.2.0: U.S. Geological Survey Software Release.

Bruno, M.C., Maiolini, B., Carolli, M., & Silveri, L. (2009). Impact of hydropeaking on hyporheic invertebrates in an Alpine stream (Trentino, Italy). *Annales De Limnologie - International Journal of Limnology*, *45*(3), 157–170.

Cardenas, M.B., Wilson, J.L., & Zlotnik, V.A. (2004). Impact of heterogeneity, bed forms, and stream curvature on subchannel hyporheic exchange. *Water Resources Research*, *40*(8).

Casas-Mulet, R., Matthews, E., Geist, J., Durance, I., & Cable, J. (2021). Negative effects of parasite exposure and variable thermal stress on brown trout (Salmo trutta) under future climatic and hydropower production scenarios. *Climate Change Ecology*, *2*, 100039.

Castagna, M., Bellin, A., & Chiogna, G. (2015). Uncertainty Estimation and Evaluation of Shallow Aquifers' Exploitability: The Case Study of the Adige Valley Aquifer (Italy). *Water*, *7*(12), 3367–3395.

Chiogna, G., Majone, B., Cano Paoli, K., Diamantini, E., Stella, E., & Mallucci, S., et al. (2016). A review of hydrological and chemical stressors in the Adige catchment and its ecological status. *The Science of the Total Environment*, *540*, 429–443.

Cho, M.S., Solano, F., Thomson, N. R., Trefry, M.G., Lester, D.R., & Metcalfe, G. (2019). Field Trials of Chaotic Advection to Enhance Reagent Delivery. *Groundwater Monitoring & Remediation*, *39*(3), 23–39.

Cirpka, O. A., Chiogna, G., Rolle, M., & Bellin, A. (2015). Transverse mixing in three-dimensional nonstationary anisotropic heterogeneous porous media. *Water Resources Research*, *51*(1), 241–260. https://doi.org/10.1002/2014WR015331

de Anna, P., Dentz, M., Tartakovsky, A., & Le Borgne, T. (2014). The filamentary structure of mixing fronts and its control on reaction kinetics in porous media flows. *Geophysical Research Letters*, *41*(13), 4586–4593.

Dentz, M., & Carrera, J. (2005). Effective solute transport in temporally fluctuating flow through heterogeneous media. *Water Resources Research*, *41*(8).

de Dreuzy, J.-R., Carrera, J., Dentz, M., & Le Borgne, T. (2012). Asymptotic dispersion for two-dimensional highly heterogeneous permeability fields under temporally fluctuating flow. *Water Resources Research*, *48*(1).

Ferencz, S.B., Cardenas, M.B., & Neilson, B.T. (2019). Analysis of the Effects of Dam Release Properties and Ambient Groundwater Flow on Surface Water-Groundwater Exchange Over a 100-km-Long Reach. *Water Resources Research*, *55*(11), 8526–8546.

Fette, M., Weber, C., Peter, A., & Wehrli, B. (2007). Hydropower production and river rehabilitation: A case study on an alpine river. *Environmental Modeling & Assessment*, *12*(4), 257–267.

Francis, B.A., Francis, L.K., & Cardenas, M.B. (2010). Water table dynamics and groundwater-surface water interaction during filling and draining of a large fluvial island due to dam-induced river stage fluctuations. *Water Resources Research*, *46*(7).

Galli, M. (2019). Effect of hydropeaking on groundwater flow in the Adige aquifer (Italy) (Master's thesis). Technical University of Munich.

Geng, X., Michael, H.A., Boufadel, M.C., Molz, F.J., Gerges, F., & Lee, K. (2020). Heterogeneity Affects Intertidal Flow Topology in Coastal Beach Aquifers. *Geophysical Research Letters*, *47*(17).

Hauer, C., Siviglia, A., & Zolezzi, G. (2017). Hydropeaking in regulated rivers - From process understanding to design of mitigation measures. *The Science of the Total Environment*, *579*, 22–26.

Kitanidis, P. K. (1994). The concept of the Dilution Index. *Water Resources Research*, *30*(7), 2011–2026.

Laio, F., Porporato, A., Ridolfi, L., & Rodriguez-Iturbe, I. (2001). Plants in water-controlled ecosystems: active role in hydrologic processes and response to water stress. *Advances in Water Resources*, *24*(7), 707–723.

Meteotrentino. (2022). *Stazioni Meteorologiche T0408 Mezzolombardo (Maso Delle Part)*. Retrieved from http://storico.meteotrentino.it/web.htm?ppbm=T0408&rs&1&df

Neupauer, R.M., Meiss, J.D., & Mays, D.C. (2014). Chaotic advection and reaction during engineered injection and extraction in heterogeneous porous media. *Water Resources Research*, *50*(2), 1433–1447.

Neupauer, R.M., Sather, L.J., Mays, D.C., Crimaldi, J.P., & Roth, E.J. (2020). Contributions of Pore-Scale Mixing and Mechanical Dispersion to Reaction During Active Spreading by Radial Groundwater Flow. *Water Resources Research*, *56*(7).

Niswonger, R. G., Panday, S., & Ibaraki, M. (2011). MODFLOW-NWT, A Newton formulation for MODFLOW-2005. *U.S. Geological Survey Techniques and Methods 6–A37*.

Pérez Ciria, T., Labat, D., & Chiogna, G. (2019). Detection and interpretation of recent and historical streamflow alterations caused by river damming and hydropower production in the Adige and Inn river basins using continuous, discrete and multiresolution wavelet analysis. *Journal of Hydrology*, *578*, 124021.

Piscopo, A.N., Neupauer, R.M., & Mays, D.C. (2013). Engineered injection and extraction to enhance reaction for improved in situ remediation. *Water Resources Research*, *49*(6), 3618–3625.

Provincia Autonoma di Trento - Ufficio Dighe. (2017). *Dati della rete di monitoraggio dell'Ufficio Dighe – Servizio Prevenzione rischi della Provincia Autonoma di Trento*. Retrieved from https://www.floods.it/public/DatiLive.php

Rodriguez-Iturbe, I., Porporato, A., Laio, F., & Ridolfi, L. (2001). Plants in water-controlled ecosystems: active role in hydrologic processes and response to water stress. *Advances in Water Resources*, *24*(7), 695–705.

Rolle, M., & Le Borgne, T. (2019). Mixing and Reactive Fronts in the Subsurface. *Reviews in Mineralogy and Geochemistry*, *85*(1), 111–142.

Sawyer, A.H., Cardenas, M.B., Bomar, A., & Mackey, M. (2009). Impact of dam operations on hyporheic exchange in the riparian zone of a regulated river. *Hydrological Processes*, *23*(15), 2129–2137.

Singh, T., Wu, L., Gomez-Velez, J.D., Lewandowski, J., Hannah, D. M., & Krause, S. (2019). Dynamic Hyporheic Zones: Exploring the Role of Peak Flow Events on Bedform-Induced Hyporheic Exchange. *Water Resources Research*, *55*(1), 218–235.

Song, X., Chen, X., Stegen, J., Hammond, G., Song, H.-S., & Dai, H., et al. (2018). Drought Conditions Maximize the Impact of High-Frequency Flow Variations on Thermal Regimes and Biogeochemical Function in the Hyporheic Zone. *Water Resources Research*, *54*(10), 7361–7382.

Song, X., Chen, X., Zachara, J.M., Gomez-Velez, J.D., Shuai, P., Ren, H., & Hammond, G.E. (2020). River Dynamics Control Transit Time Distributions and Biogeochemical Reactions in a Dam-Regulated River Corridor. *Water Resources Research*, *56*(9).

Sposito, G. (2006). Chaotic solute advection by unsteady groundwater flow. *Water Resources Research*, *42*(6).

Tang, Q., Kurtz, W., Brunner, P., Vereecken, H., & Hendricks Franssen, H.-J. (2015). Characterisation of river–aquifer exchange fluxes: The role of spatial patterns of riverbed hydraulic conductivities. *Journal of Hydrology*, *531*, 111–123.

Trefry, M.G., Lester, D.R., Metcalfe, G., & Wu, J. (2019). Temporal Fluctuations and Poroelasticity Can Generate Chaotic Advection in Natural Groundwater Systems. *Water Resources Research*, *55*(4), 3347–3374.

Valocchi, A.J., Bolster, D., & Werth, C.J. (2019). Mixing-Limited Reactions in Porous Media. *Transport in Porous Media*, *130*(1), 157–182.

Wright, E.E., Richter, D.H., & Bolster, D. (2017). Effects of incomplete mixing on reactive transport in flows through heterogeneous porous media. *Physical Review Fluids*, *2*(11).

Wu, J., Lester, D.R., Trefry, M.G., & Metcalfe, G. (2020). When Do Complex Transport Dynamics Arise in Natural Groundwater Systems? *Water Resources Research*, *56*(2).

Ye, Y., Chiogna, G., Lu, C., & Rolle, M. (2020). Plume deformation, mixing, and reaction kinetics: An analysis of interacting helical flows in three-dimensional porous media. *Physical Review. E*, *102*(1-1), 13110.

Zachara, J.M., Chen, X., Murray, C., & Hammond, G. (2016). River stage influences on uranium transport in a hydrologically dynamic groundwater-surface water transition zone. *Water Resources Research*, *52*(3), 1568–1590.

Ziliotto, F., Basilio Hazas, M., Rolle, M., & Chiogna, G. (2021). Mixing Enhancement Mechanisms in Aquifers Affected by Hydropeaking: Insights From Flow-Through Laboratory Experiments. *Geophysical Research Letters*, *48*(21).

Zolezzi, G., Siviglia, A., Toffolon, M., & Maiolini, B. (2011). Thermopeaking in Alpine streams: event characterization and time scales. *Ecohydrology*, *4*(4), 564–576.